

\*\*Volume Title\*\*  
 ASP Conference Series, Vol. \*\*Volume Number\*\*  
 \*\*Author\*\*  
 © \*\*Copyright Year\*\* Astronomical Society of the Pacific

## The Stability of Galaxy Disks

Kyle B. Westfall,<sup>1</sup> David R. Andersen,<sup>2</sup> Matthew A. Bershady,<sup>3</sup> Thomas P. K. Martinsson,<sup>4</sup> Robert A. Swaters,<sup>5</sup> & Marc A. W. Verheijen<sup>1</sup>

<sup>1</sup>*Kapteyn Astronomical Institute, University of Groningen*

<sup>2</sup>*NRC Herzberg Institute of Astrophysics*

<sup>3</sup>*Department of Astronomy, University of Wisconsin-Madison*

<sup>4</sup>*Leiden Observatory, Leiden University*

<sup>5</sup>*National Optical Astronomy Observatory*

**Abstract.** We calculate the stellar surface mass density ( $\Sigma_*$ ) and two-component (gas+stars) disk stability ( $Q_{\text{RW}}$ ) for 25 late-type galaxies from the DiskMass Survey. These calculations are based on fits of a dynamical model to our ionized-gas and stellar kinematic data performed using a Markov Chain Monte Carlo sampling of the Bayesian posterior. Marginalizing over all galaxies, we find a median value of  $Q_{\text{RW}} = 2.0 \pm 0.9$  at 1.5 scale lengths. We also find that  $Q_{\text{RW}}$  is anti-correlated with the star-formation rate surface density ( $\dot{\Sigma}_*$ ), which can be predicted using a closed set of empirical scaling relations. Finally, we find that the star-formation efficiency ( $\dot{\Sigma}_*/\Sigma_g$ ) is correlated with  $\Sigma_*$  and weakly anti-correlated with  $Q_{\text{RW}}$ . The former is consistent with an equilibrium prediction of  $\dot{\Sigma}_*/\Sigma_g \propto \Sigma_*^{1/2}$ . Despite its order-of-magnitude range, we find no correlation of  $\dot{\Sigma}_*/\Sigma_g \Sigma_*^{1/2}$  with any other physical quantity derived by our study.

**Motivation:** Studies of the star-formation law in disk galaxies have largely focused on assessments of the gaseous component (e.g., Kennicutt 1998). This approach is understandable given that it is the gas from which stars are formed. However, the stellar component is also relevant; for example, it is often the dominant contributor to the gravitational potential in the disk plane. Indeed, a relation between the star-formation efficiency (SFE; the star-formation rate per unit gas mass) and the stellar surface mass density ( $\Sigma_*$ ) has been found empirically (Shi et al. 2011) and is expected theoretically (Ostriker et al. 2010).

The theory presented by Ostriker et al. (2010) is derived assuming an equilibrium of the diffuse and self-gravitating gas with respect to its thermal properties and the pressure balance within the vertical gravitational field of the disk. Depending on the relevant timescales, this equilibrium may not be reached in galaxies that exhibit modal potential perturbations (e.g. spiral arms). In so far as the two-component disk stability ( $Q_{\text{RW}}$ ; see below) quantifies the susceptibility of a disk to such perturbations, it is therefore interesting to test the validity of the equilibrium prediction in disks of different  $Q_{\text{RW}}$ .

The primary systematic uncertainties in most extant calculations of  $\Sigma_*$ , and  $Q_{\text{RW}}$ , are incurred via the use of stellar-population-synthesis models (e.g. Leroy et al. 2008). In contrast, the high-resolution stellar kinematic data from the DiskMass Survey (Bershady et al. 2010a) allow for a *dynamical* calculation of  $\Sigma_*$ , which is not subject to the same sys-

tematic errors. Therefore, we use these data to investigate the correlation of  $\dot{\Sigma}_*$  and SFE with  $\Sigma_*$  and  $Q_{\text{RW}}$ .

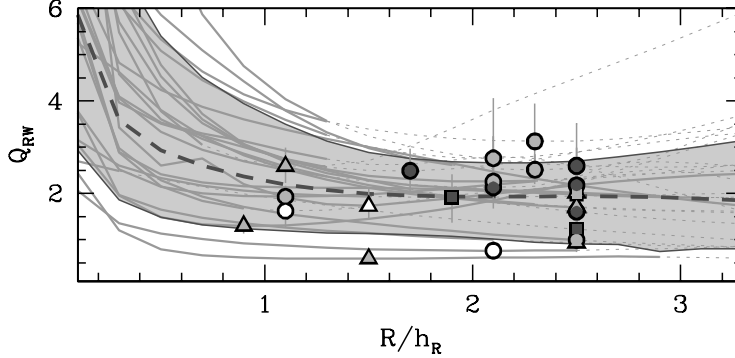


Figure 1. The two-component disk stability,  $Q_{\text{RW}}$ , as a function of  $R/h_R$  from the dynamical model of each galaxy. The profile for each galaxy transitions from the solid- to dotted-gray lines at the radius when the model is no longer directly constrained by our LOS stellar velocity dispersions, only by the rotation curves. The minimum  $Q_{\text{RW}}$  within  $2.5 h_R$ ,  $Q_{\text{RW}}^{\text{min}}$ , is marked for each galaxy: light-gray is used for “bc” and “c” type spirals; white and dark-gray are used for earlier and later Hubble types, respectively. Circles, triangles, and squares are for unbarred (S), weakly barred (SAB), and barred (SB) galaxies, respectively. The dark-gray dashed line is the median  $Q_{\text{RW}}$  from the marginalized distributions at each  $R/h_R$ , and the light-gray region is the 68% confidence interval.

**Measurements:** Detailed discussions of our dynamical assumptions can be found in papers from the DiskMass Survey series (e.g., Bershady et al. 2010b; Westfall et al. 2011; Martinsson et al. 2013). Briefly, we calculate the dynamical surface mass density,  $\Sigma_{\text{dyn}} \propto \sigma_z^2/h_z$ , assuming a parallel-plane disk with an exponential vertical density profile (van der Kruit 1988). To calculate the scale height ( $h_z$ ), we use a scaling relation between the disk oblateness ( $h_R/h_z$ ) and its scale length ( $h_R$ ) based on observations of edge-on spirals (Bershady et al. 2010b). To obtain the vertical velocity dispersion ( $\sigma_z$ ), we fit a dynamical model to our line-of-sight (LOS) kinematic data that yields the shape of the stellar velocity ellipsoid. We obtain  $\Sigma_*$  by subtracting the gas mass surface density,  $\Sigma_g = 1.4(\Sigma_{\text{H}_2} + \Sigma_{\text{HI}})$ , from  $\Sigma_{\text{dyn}}$ . Finally, we calculate the Toomre (1964) stability criterion,  $Q_i \propto \kappa \sigma_{R,i}/\Sigma_i$ , for the gas and stars individually based on the results of the dynamical model and combine them into a two-component stability ( $Q_{\text{RW}}$ ) following Romeo & Wiegert (2011);  $\kappa$  is the epicyclic frequency, and the cold-gas velocity dispersion is assumed to be isotropic and half of the ionized-gas dispersion. The assumptions made by the dynamical model are very similar to those from Westfall et al. (2011), but the methodology follows Bayesian statistics (see Westfall et al., *in prep*).

Figure 1 shows  $Q_{\text{RW}}(R)$  for each galaxy individually and when marginalized over all galaxies. The marginalized  $Q_{\text{RW}}$  is large toward the center ( $\kappa$  is largest in the rising part of the rotation curve) and then asymptotes to a nearly constant value at  $R > 1h_R$ ; the median of the marginalized probability distribution is  $Q_{\text{RW}} = 2.0 \pm 0.9$  at  $R = 1.5h_R$ .

**Anti-correlation Between Stability and Star-formation Activity:** We calculate  $\dot{\Sigma}_{e,*} = \dot{M}_*/\pi R_{25}^2$  using star-formation rates ( $\dot{M}_*$ ) based on 21-cm radio-continuum measurements and the calibrations from Yun et al. (2001), where  $R_{25}$  is the radius of the  $\mu_B = 25$  mag arcsec $^{-2}$  surface-brightness isophote. The results are compared with  $Q_{\text{RW}}$  at  $1.5h_R$

( $Q_{\text{RW}}^{1.5h_R}$ ) in Figure 2a. The Spearman rank-correlation coefficient,  $r_s$ , demonstrates that the two quantities are anti-correlated; however, the correlation is only roughly three times its measurement error, as estimated using bootstrap simulations. The anti-correlation strengthens to  $r_s = -0.53 \pm 0.14$  if we instead consider the minimum  $Q_{\text{RW}}$  within  $R \leq 2.5h_R$  ( $Q_{\text{RW}}^{\text{min}}$ ; see Figure 1). The anti-correlation between  $\dot{\Sigma}_{e,*}$  and  $Q_{\text{RW}}$  can be predicted based on empirical scaling relations.

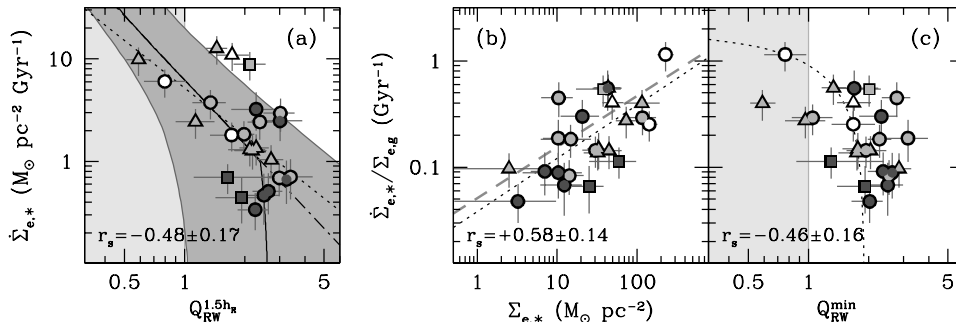


Figure 2. (a) Measurements of  $\dot{\Sigma}_{e,*}$  and  $Q_{\text{RW}}^{1.5h_R}$  for our galaxies with the nominal disk instability region in light-gray. Colors and symbol types are the same as in Figure 1. The solid black line is the predicted correlation based on empirical scaling relations when using the average properties of our sample; the dark-gray region encompasses results found when using the parameters appropriate for each galaxy. The dotted line is the expectation from Li et al. (2006) with an optimal normalization for our data. (b) SFE versus  $\Sigma_{e,*}$  and (c) SFE versus  $Q_{\text{RW}}^{\text{min}}$ . See text for more description.

The details of the scaling-relation calculation will be presented by Westfall et al. (*in prep*). In short, we define a set of auxiliary parameters — cold-gas dispersion,  $\sigma_g$ ; central disk surface brightness in  $K$ -band,  $\mu_{0,K}$ ;  $K$ -band mass-to-light ratio,  $\Upsilon_K$ ;  $h_R$ ;  $R_{25}$ ; and  $\alpha = \sigma_z/\sigma_R$  — that, for a given  $\dot{M}_*$ , can be used to determine the input quantities required in the calculation of  $Q_{\text{RW}}(R)$  —  $\kappa$ ,  $\sigma_g$ ,  $\sigma_R$ ,  $\Sigma_g$ , and  $\Sigma_*$ . For the black line in Figure 2a, we use the Kennicutt-Schmidt law (Kennicutt 1998) to determine the average  $\Sigma_g$  within  $R_{25}$  for a given  $\dot{\Sigma}_{e,*}$  and distribute that gas according to the  $\Sigma_g(R)$  profile from Bigiel & Blitz (2012). We assume a hyperbolic tangent form for the circular speed — used to get  $\kappa$  (Binney & Tremaine 2008) — with parameters that follow the scaling relations with the light profile from Andersen & Bershady (2013), and yields a ratio with a disk-only rotation curve — the disk maximality — in accordance with the surface brightness dependence found by Martinsson et al. (2013). The inflection of the result seen at  $Q_{\text{RW}}^{1.5h_R} > 2$  is due to the stellar disk becoming less stable than the gas disk. For  $Q_{\text{RW}}^{1.5h_R} < 2$ , the predicted relation is very well described by a power-law slope of -2.07 (dot-dashed line), which is steeper than the slope of -1.54 predicted by Li et al. (2006).

For Figures 2b and 2c, we calculate “effective” mass surface densities ( $\Sigma_{e,g}$  and  $\Sigma_{e,*}$ ) by integrating the stellar and gas mass profiles from our dynamical model to  $R_{25}$  and dividing by the total surface area. The Figures show the SFE ( $\dot{\Sigma}_{e,*}/\Sigma_{e,g}$ ) as a function of  $\Sigma_{e,*}$  and  $Q_{\text{RW}}^{\text{min}}$ . The SFE is correlated with  $\Sigma_{e,*}$  and has a power-law dependence that is in agreement with the empirical findings of Shi et al. (2011, gray dashed line; see their equation 6) and the theoretical prediction of Ostriker et al. (2010, black dotted line;  $\dot{\Sigma}_{e,*}/\Sigma_{e,g} \propto \Sigma_{e,*}^{1/2}$ , where we have optimized the normalizing constant). Contrary to previous results (Leroy et al. 2008), we also find an albeit weak anti-correlation be-

tween the SFE and the minimum disk stability. This anti-correlation is consistent with the expected *linear* relationship from Li et al. (2006, dotted line with a best-fitting intercept), but far from verifies it due to the scatter in the data.

**Conclusion:** Our analysis of the kinematic data from the DiskMass Survey yields a significant anti-correlation between the star-formation activity of a disk and its gravitational stability. However, we also find that our data are consistent with the equilibrium solution derived by Ostriker et al. (2010), with no significant correlation between  $\dot{\Sigma}_{e,*}/\Sigma_{e,g}\Sigma_{e,*}^{1/2}$  and any other quantity in our analysis. In so far as disk stability quantifies the susceptibility of a disk to modal potential perturbations (bars, spiral arms, etc.), this result suggests that such perturbations may not prohibit this proposed equilibrium. We find an error-weighted geometric mean of  $\langle \log(\dot{\Sigma}_{e,*}/\Sigma_{e,g}\Sigma_{e,*}^{1/2}) \rangle = -3.25 \pm 0.27$  in units of  $(G/\text{pc})^{1/2}$ , where  $G = 4.30 \times 10^{-3} (\text{km/s})^2 \text{ pc } \mathcal{M}_{\odot}^{-1}$  is the gravitational constant. However, there is an order-of-magnitude range in  $\dot{\Sigma}_{e,*}/\Sigma_{e,g}\Sigma_{e,*}^{1/2}$  among the galaxies in our sample. It is of great interest to understand this scatter.

**Acknowledgments.** Support for this work was provided by the National Science Foundation (AST-0307417, AST-0607516, OISE-0754437, and AST-1009491), the Netherlands Organisation for Scientific Research (614.000.807), NASA/*Spitzer* grant GO-30894, the Netherlands Research School for Astronomy, and the Leids Kerkhoven-Bosscha Fonds.

## References

- Andersen, D. R., & Bershady, M. A. 2013, ApJ, 768, 41  
 Bershady, M. A., Verheijen, M. A. W., Swaters, R. A., Andersen, D. R., Westfall, K. B., & Martinsson, T. 2010a, ApJ, 716, 198  
 Bershady, M. A., Verheijen, M. A. W., Westfall, K. B., Andersen, D. R., Swaters, R. A., & Martinsson, T. 2010b, ApJ, 716, 234  
 Bigiel, F., & Blitz, L. 2012, ApJ, 756, 183  
 Binney, J., & Tremaine, S. 2008, Galactic Dynamics: Second Edition (Princeton University Press, Princeton, NJ USA)  
 Kennicutt, R. C., Jr. 1998, ApJ, 498, 541  
 Leroy, A. K., Walter, F., Brinks, E., Bigiel, F., de Blok, W. J. G., Madore, B., & Thornley, M. D. 2008, AJ, 136, 2782  
 Li, Y., Mac Low, M.-M., & Klessen, R. S. 2006, ApJ, 639, 879  
 Martinsson, T. P. K., Verheijen, M. A. W., Westfall, K. B., Bershady, M. A., Andersen, D. R., & Swaters, R. A. 2013, A&A, 557, A131  
 Ostriker, E. C., McKee, C. F., & Leroy, A. K. 2010, ApJ, 721, 975  
 Romeo, A. B., & Wiegert, J. 2011, MNRAS, 416, 1191  
 Shi, Y., Helou, G., Yan, L., Armus, L., Wu, Y., Papovich, C., & Stierwalt, S. 2011, ApJ, 733, 87  
 Toomre, A. 1964, ApJ, 139, 1217  
 van der Kruit, P. C. 1988, A&A, 192, 117  
 Westfall, K. B., Bershady, M. A., Verheijen, M. A. W., Andersen, D. R., Martinsson, T. P. K., Swaters, R. A., & Schechtman-Rook, A. 2011, ApJ, 742, 18  
 Yun, M. S., Reddy, N. A., & Condon, J. J. 2001, ApJ, 554, 803